Simulation of Cumulative Exposure Statistics for Blast Pressure Transmission Into the Brain

X. Gary Tan, PhD; Peter Matic, PhD**

ABSTRACT Introduction: This study develops and demonstrates an analysis approach to understand the statistics of cumulative pressure exposure of the brain to repetitive blasts events. Materials and Methods: A finite element model of blast loading on the head was used for brain model biomechanical responses. The cumulative pressure exposure fraction (CPEF), ranging from 0.0 to 1.0, was used to characterize the extent and repetition of high pressures. Monte Carlo simulations were performed to generate repetitive blast cumulative exposures. Results: The blast orientation effect is as influential as the blast overpressure magnitudes. A 75° (from the side) blast orientation can produce CPEF values exceeding traumatic brain injury pressure thresholds >0.95 while, for the same blast overpressure, a 0° (front) blast orientation results in a CPEF <0.25. Monte Carlo results for different sequences reflecting notional operational and training environments show that both mean values and standard deviations of CPEF reach the statistically equilibrium state at a finite value of *n* exposures for each sequence. Conclusions: Statistical convergence of the brain pressure response metrics versus number of blasts for different exposures characterizes the transitions from "low" to "high" number of blasts and quantitatively highlights the differences between operational and training exposures.

INTRODUCTION

In recent military operations, large number of service members were diagnosed with repetitive concussive or subconcussive brain injury due to explosive blast exposure.[1] Moreover, military personnel including explosive breachers and weapons crews are subjected to repeated blast wave exposures as part of routine combat training.[2] Repetitive exposure to blast waves, in operational or training environments, can subject the warfighter to different sequences of pressures and incident directions of these waves generated from characteristic ranges of these parameters. Military personnel experiencing repeated exposures may experience neurological disorders, including concentration problems, blurred vision, irritability, headaches, dizziness, fatigue, sleep disorders, and depression.[3,4] Furthermore, many studies have provided evidence that the effects of blast exposure on the brain are cumulative and long-lasting, which result in the acceleration of aging process of the brain.[5]

Blast pressure transmission into the brain is a complex sequence of events associated with traumatic brain injuries (TBIs).[6] Current understanding of blast-induced brain injury mechanisms is limited.[7,8] In particular, cumulative head injury effect by the repetitive blasts over a prolonged period has been studied[9,10] but is not well understood.[11] Clinical research of mild TBIs (mTBIs) in humans is limited to post-trauma studies.[12] Existing animal models cannot directly correlate the injury with humans.[13] Most cases of blast neurotrauma, resulting in structural, biochemical, or electrical abnormalities in the brain, spinal cord, or other nerves, are mild (concussion)[14] and are difficult to detect with conventional neuroimaging.[15] In a postmortem study of veterans exposed to blast injury, Goldstein et al. found evidence of a τ protein-linked degenerative brain disease known as chronic traumatic encephalopathy (CTE).[13] The researchers also found that repetitive blast exposure in mice damages the blood-brain barrier and causes brain inflammation.[16,17]

Blast sensors promise to record and characterize individual and multiple external blast pressure environments including incident overpressure and orientation.[18] The value of blast sensor information will be increased by a better understanding of the statistics of the dynamic internal brain pressures and the transition from a sequence dependent "low number of blasts" to a sequence independent "high number of blasts." Quantitative metrics describing the internal pressures generated in the brain from repetitive blasts should support better injury diagnosis, risk management, and protective strategies.[19] Computational analyses of blast wave biomechanics have the ability to establish relationships between the blast pressure on the head, internal biomechanical response, and locations of induced brain injury. This insight can be useful in understanding injury mechanisms and designing improvement of protection systems.[20]

The objective of this effort, motivated and guided by physical measurements and computational analyses reported to date, was to employ Monte Carlo simulation of multiple blast events, compile predicted internal brain dynamic pressures

*Materials Science and Technology Division (Code 6300), U.S. Naval Research Laboratory, 4555 Overlook Ave SW, Washington, DC 20375

Presented as a poster at the 2018 Military Health System Research Symposium. MHSRS abstract number: MHSRS-18-1406.

The views expressed in this paper are those of the authors and do not necessarily represent the official position or policy of the U.S. Government, the Department of Defense, or the Department of the Navy.

This material is declared a work of the U.S. Government and is not subject to copyright protection in the United States. Approved for public release; distribution is unlimited.

doi:10.1093/milmed/usz308

Published by Oxford University Press on behalf of the Association of Military Surgeons of the United States 2020. This work is written by (a) US Government employee(s) and is in the public domain in the US.

Downloaded from https://academic.oup.com/milmed/article/185/Supplement_1/214/5740777 by guest on 19 April 2022

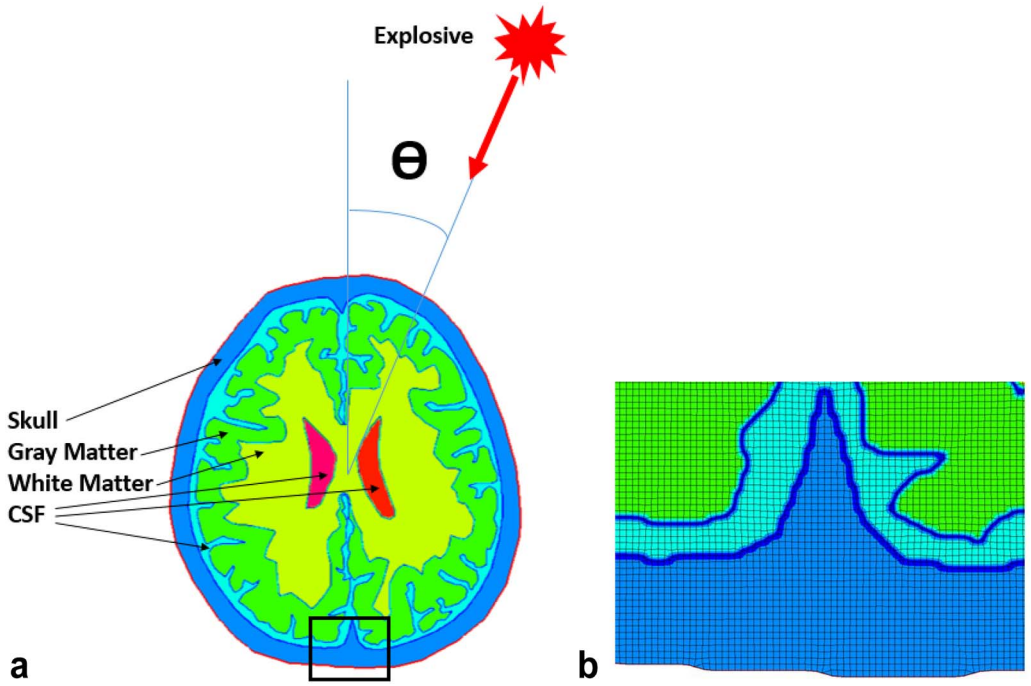


FIGURE 1. (a) A 2D slice in transverse/axial plane of head and (b) zoom-in at the bottom of head with the mesh.

TABLE I. Mechanical Properties Used in Human Head FE Model

Tissue	Material	Constants	Mass Density, kg/m^3
Skull	Linear elastic	$E = 6.5$ GPa, $\nu = 0.3$	1,100
Gray matter	Viscoelastic	$\kappa = 2.19$ GPa, $G_0 = 8$ kPa, $G_1 = 6.5$ kPa, $\tau = 25$ ms	1,040
White matter	Viscoelastic	$\kappa = 2.19$ GPa, $G_0 = 10.4$ kPa, $G_1 = 8.4$ kPa, $\tau = 25$ ms	1,040
CSF	Hyperelastic	$\kappa = 2.19$ GPa, $G = 1$ kPa	1,000

for random sequences of blast events, and characterize the transition from "low" to "high" numbers of blast exposures based on the statistics. Direct simulation of individual blast events constituting training or operational blast sequences, using three-dimensional (3D) blast and head fluid structure interaction models, would be computationally cost intensive. The approach taken here to demonstrate the approach uses a combination of detailed computational simulations, probabilistic calculations using the detailed results database and statistical analysis of the generated data for blast sequences.

A small number of more demanding detailed computational simulations are used to generate a database of representative results for combinations of blast overpressures and incident directions. The database is queried for the probabilistic analysis of long sequences of $N_{\text{tot}} = 200$ blasts, which can represent operational or training exposures. The statistics of the internal brain pressure responses are then analyzed to identify and quantify their initial variability early in the blast sequences and their subsequent convergence trends later in the blast sequences for operational and training exposures.

METHODS

Computational Finite Element Model of Human Head

A transverse 2D section (axial plane) from a 3D human head model is used to illustrate method. The 3D head was generated from in vivo magnetic resonance imaging scans with 1 mm isotropic resolution of a young adult male.[21,22] An in-house meshing tool was used to generate a high-quality quadrilateral mesh (Fig. 1). The distance from the left to right is 164 mm and from the anterior to posterior is 184 mm. The mesh consists of four different materials, that is, gray matter, white matter, cerebrospinal fluid (CSF), and skull. An average element size of 0.5 mm is used to capture the complex shapes of sulci and gyri and the high-frequency response due to the blast loading. The total number of elements exceeds 100,000.

The material models and corresponding parameters are shown in Table I.[23] The gray matter and white matter were modeled as an isotropic viscoelastic material. The CSF between the skull and brain and in ventricles was modeled as hyperelastic solids with a low shear modulus. The skull

Downloaded from https://academic.oup.com/milmed/article/185/Supplement_1/214/5740777 by guest on 19 April 2022

TABLE II. Pressure-Based Thresholds of Blast-Induced TBI[22]

Blast-Induced TBI Type	Repetitive mTBI	Single Onset mTBI	Single Moderate TBI
Threshold (kPa)	142	173	204

TABLE III. ConWep Spherical Free-Air Blasts With Standoff Distance of 2.7 m From the Head

Case	TNT Mass (kg)	Peak Incident Overpressure (psi/kPa)	Positive-Phase Duration (ms)	Time of Arrival (ms)
1	0.36	7.5/51.71	2.139	4.175
2	0.57	10/68.95	2.324	3.796
3	0.79	12.5/86.18	2.443	3.521
4	1.03	15/103.42	2.517	3.302

was assumed to behave as a linear elastic material because of the small strain experienced during the blast.

The multiphysics code CoBi[24] finite element (FE) solver is adopted for the simulation of blast-induced biomechanical response. The ConWep[25] model is used to generate the transient blast loading resulting from a free-field explosion in air (without the ground effect). A trinitrotoluene (TNT) charge is detonated at a distance of 2.7 m and with an orientation angle θ relative to the middle sagittal plane of the head. This produces a specified incident overpressure near the head.

Each FE simulation, for a specified incident blast overpressure and orientation combination, generates the dynamic response of the head model over a 2.5 ms duration. The resulting spatially and temporally resolved dynamic internal pressure fields in the brain model are compared on an element-by-element basis to threshold values associated with different levels of TBI. Incremental TBI thresholds of 142, 173, and 204 kPa, adapted from the literature,[26] were used to assess the specific levels of TBI (Table II). If the maximum pressure in an element crosses any TBI threshold, the element is considered to have been "injured." (Although the exact mechanism of brain injury from a blast overpressure or a shock front is not clearly understood, pressure values are one quantity useful for characterizing the dynamic response of the brain tissues.)

Monte Carlo Simulation of Repetitive Blast Sequences

The Monte Carlo simulations of repetitive blast cumulative exposures were generated from random sequences of 200 blast overpressure and orientation pairs. These pairs are used to query a reference database constructed from the head model FE simulation results for 96 different loading configurations. These loading configurations are constructed from 4 incident blast overpressures and 24 blast orientation angles.

The four peak incident overpressures are 7.5, 10.0, 12.5, and 15.0 psi (51.71, 68.95, 86.18, and 103.42 kPa). These overpressure values span a range covering training and survivable operational blasts. TNT masses used to generate these overpressures covering the training and operational scenarios are shown in Table III. The 24 orientation angles θ range from 0 to 360° in increments of 15°. The TBI threshold criterion values are applied to the results of each simulation in the database to construct the corresponding exposure maps of the brain exceeding the pressure thresholds.

Three notional repetitive blast exposure environments, relevant to three service communities, were constructed for the probabilistic analyses from the results database. The random sequences are drawn from the overpressure and orientation domain as shown schematically in Figure 2. An operational/-combat exposure environment covers all four incident overpressures and all 24 angles from −180 to +180°. This represents a less predictable overpressure environment. A breacher training blast exposure environment covers three lower incident overpressures from 7.5 to 12.5 psi (51.71–86.18 kPa) and five angles from −30 to 30°. These 15 cases represents a more structured and controlled overpressure blast environment. An intermediate mixed exposure environment was constructed from 68 cases covering all four incident overpressures but only a 17-angle subset from −120 to 120°.

For each of the three repetitive blast loading environments, $S = 20$ random sequences of $N_{tot} = 200$ blast overpressure-orientation configurations were generated. Each blast $n = 1,2,3, \ldots,198,199,200$ in a random sequence refers back to the precomputed database containing the dynamic responses of the head calculated from the FE models.

The pressure exposure (PE) to an element in the FE model is defined as PE(e, n) where e is the element in the brain model and n is one blast event in the random sequence. V(e) is the associated element volume. PE = 1 if the pressure in the element equals or exceeds an injury threshold pressure (Table II) at any time during the simulation. PE = 0 if the element pressure does not exceed an injury threshold.

It follows that the cumulative pressure exposure fraction CPEF(e, N) for each element e in the brain model after N blast

Downloaded from https://academic.oup.com/milmed/article/185/Supplement_1/214/5740777 by guest on 19 April 2022

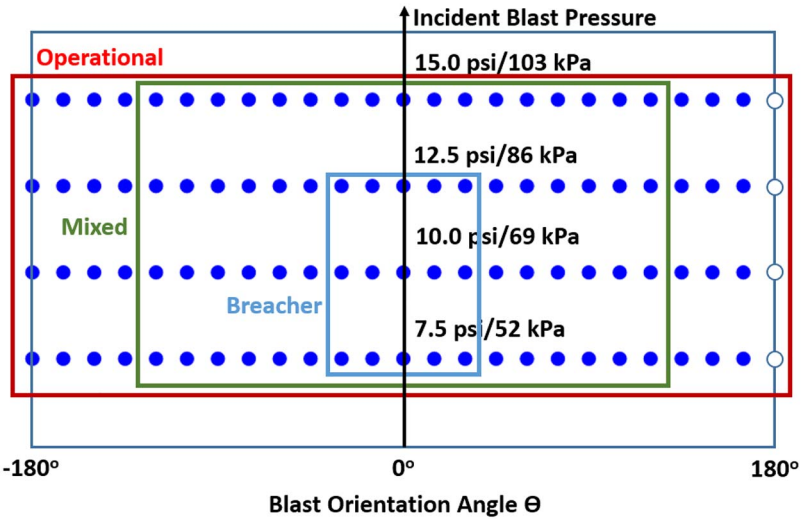


FIGURE 2. Range of notional incident overpressure and orientation sets for breacher, mixed, and operational blast exposures.

events ($1 \leq N \leq N_{\text{tot}}$) is defined as

$$\text{CPEF}(e,N) = \frac{\sum_{n=1}^{N} \text{PE}(e,n) \times V(e)}{N \times V(e)} = \frac{\sum_{n=1}^{N} \text{PE}(e,n)}{N}$$

Then, the CPEF (E_{tot}, N) for the entire brain of E_{tot} elements after N blast events is defined as

$$\text{CPEF}(E_{\text{tot}},N) = \frac{\sum_{n=1}^{N} \sum_{e=1}^{E_{\text{tot}}} \text{PE}(e,n) \times V(e)}{N \times \sum_{e=1}^{E_{\text{tot}}} V(e)}$$

This is the sum of all pressures exceeding a specified injury threshold, weighted by the volume of each element, normalized by the total brain volume, and number of blast events. Therefore, CPEF(E_{tot}, N) has a value between 0 and 1.

RESULTS

Dynamic Pressure Response of the Head Subjected to Blast

Blast pressure transmission into the brain from the skull surface is a complex dynamic event. Figures 3–5 show, for example, the pressure field evolving in the head between 0 and 0.25 ms for the incident overpressure of 15 psi (103.42 kPa) and blast orientation angles of 0, 90, and 180°. The propagation of the pressure waves into the skull and interior soft materials can be seen. Because of similar acoustic impedance between the CSF and brain, the pressure propagates smoothly at the interface between the CSF and brain. Pressure waves travel faster in the skull than in the brain due to the difference in the wave propagation speeds. The skull experiences bending modes in which the stress across the skull thickness varies from compression to tension.

The positive pressure (ie, compression) propagates into the brain first. After 0.12 ms, the negative pressure (ie, tension) begins to develop at the contrecoup of the brain. The size of the coup pressure and the intensity of the contrecoup negative pressure differ among the three orientations.

The highest values of coup pressures at 0° incidence (Fig. 3) are confined to a small focal area near the front of the head over the first 0.12 ms. A qualitatively similar behavior at the back of the head occurs for 180° incidence (Fig. 5), with somewhat longer persistence at lower pressures to 0.25 ms. For 90° incidence (Fig. 4), however, the high pressure area is significantly larger and persistent out to 0.25 ms.

All three orientations generate a clear negative-to-positive pressure contrecoup pattern between 0.16 and 0.20 ms. The 0 and 180° orientations generate well-defined contrecoup focal areas, while the pattern for the 90° orientation is more diffuse and less focal, likely due to the larger and more persistent high pressure area on the coup side.

These observations on the brain dynamic pressure patterns for these three orientations are significant toward understanding and quantifying repetitive exposure statistics for pressures exceeding injury thresholds. In Figure 6, the CPEF parameter is plotted parametrically for a single 15 psi (103.42 kPa) overpressure, all 24 orientations, and 3 injury pressure thresholds. The plot quantifies that the CPEF increases as the injury threshold decreases. It is broadly symmetric and features significant regions of both higher and lower CPEF values. The slight asymmetry in the plot is caused by the natural asymmetry of the brain anatomy used to generate the model.

Orientation intervals between (−105, −60) and (+60, +105) degrees have the highest CPEF values, while (−45, +45) and (+135, −135) degrees have the lowest values. The intervals between (−135, −105), (−60, −45), (+45, +60), and (+105, +135) degrees are the strong transition regions between the lowest and highest CPEF values.

Downloaded from https://academic.oup.com/milmed/article/185/Supplement_1/214/5740777 by guest on 19 April 2022

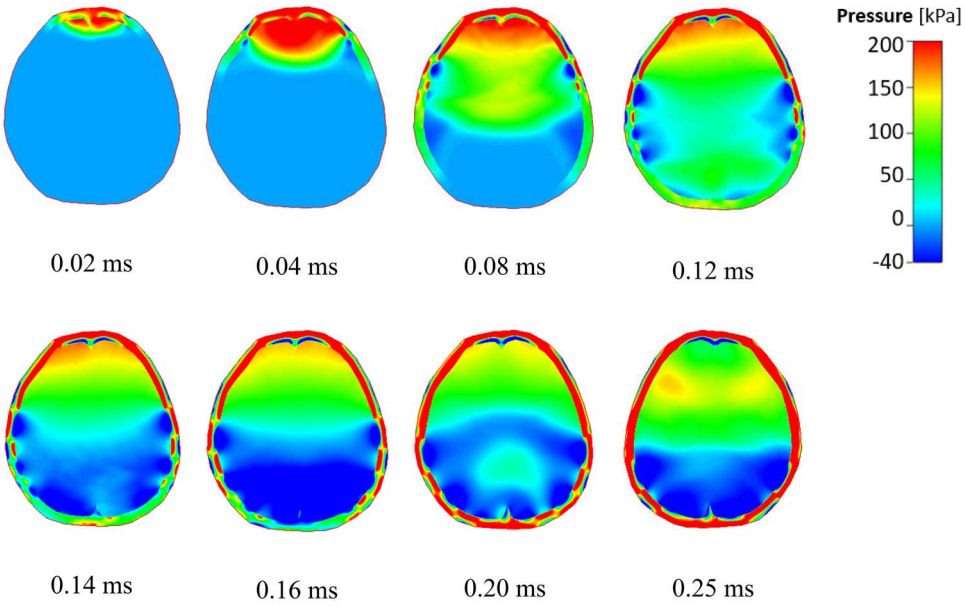


FIGURE 3. Dynamic pressures in head from single blast event at orientation angle of 0° and with incident overpressure of 15.0 psi (103 kPa).

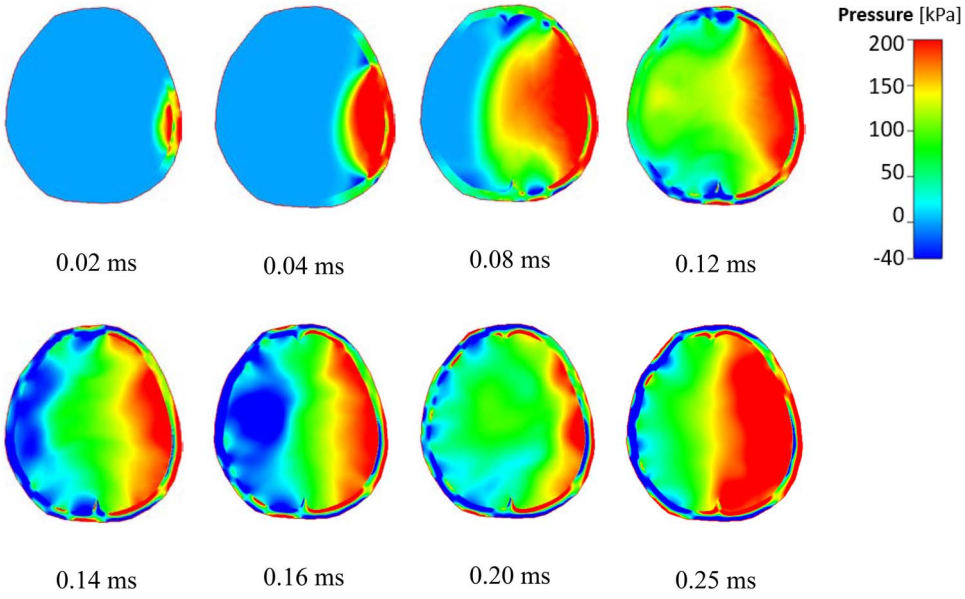


FIGURE 4. Dynamic pressures in head from single blast event at orientation angle of 90° and with incident overpressure of 15.0 psi (103 kPa).

Injury fractions of 1.0 (ie, injury throughout the brain) begin to occur between (−105, −75) and (60, 105) degree intervals for the 173 kPa injury threshold and expand to (−120, −60) and (60, 120) for the 142 kPa threshold.

The side blast orientations produce much higher injury fractions in the brain compared to frontal or rear blasts. Review of the database showed that the blast orientation of +75 (or equivalently −75) degrees causes the most damage in the brain. The corresponding dynamic pressure sequence in the head is shown in Figure 7. It shows a particularly deep coup pattern extending well across the midline of the head while retaining the large area and long-time persistence characteristic of side blasts.

The effects of increasing incident blast overpressure (from 7.5 to 15.0 psi [51.71–103.42 kPa]) on the maximum pressure in the brain for a single blast at angle of 0° are shown in Figure 8. With the higher incident overpressure, more regions in the brain reach higher pressures and thus potentially more severe injury. Note that coup and contrecoup regions are more susceptible to the higher pressures than other regions.

The effects of five blast orientations (0, 45, 90, 135, and 180°) on maximum pressures experienced in the brain for a single blast with incident overpressure of 15 psi (103.42 kPa) are shown in Figure 9. For 0, 135, and 180° blast orientations, the highest pressures reside in the region close to the coup and contrecoup. For the 45 and 90°, the corresponding side of

Downloaded from https://academic.oup.com/milmed/article/185/Supplement_1/214/5740777 by guest on 19 April 2022

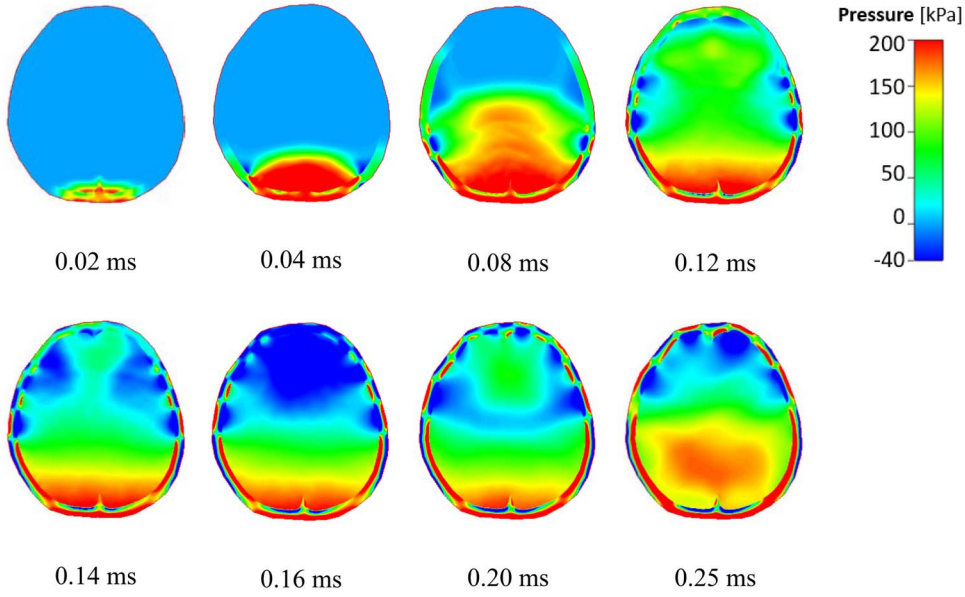


FIGURE 5. Dynamic pressures in head from single blast event at orientation angle of 180° and with incident overpressure of 15.0 psi (103 kPa).

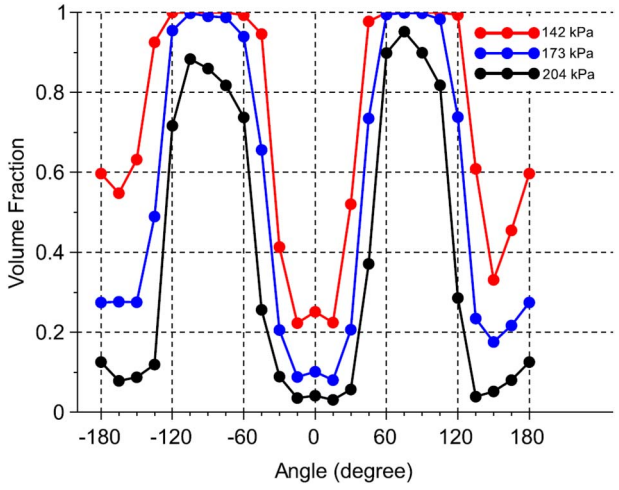


FIGURE 6. CPEF(E_{tot}, $N = 1$) versus incident blast orientation angle for single incident blast overpressure of 15.0 psi (103 kPa) and TBI thresholds of 142, 173, and 204 kPa.

the brain experiences higher maximum pressures over a larger area and deeper locations in the brain.

Role of Skull Curvature on Dynamic and Maximum Pressures in the Brain

Compared to the higher curvatures of the anterior and posterior skull, the lateral surfaces of the head exhibit much lower curvatures. Simple computational models can be used to illustrate curvature as a significant factor affecting the level of pressure infiltrations into the brain.

Two simplified 2D head models were generated with brain areas comparable to the actual head model. The first model has a circular form of radius 80 mm defining the brain area. The second model is a composite geometry composed of two semicircular shapes, each radius 70 mm, connected by a rectangle of length 33.7 mm. Both models are composed of the same three materials: skull with thickness of 7 mm, CSF layer with thickness of 5 mm, and brain filling the interior area. The same properties as listed in Table I were used. The same blast loading condition of the explosive mass of 1.03 kg at a distance of 2.7 m was applied to both models.

Figure 10 shows the peak pressures experienced in the brain during the blast loading for the circular model and the composite model in two orthogonal orientations. The curved surfaces of both models, when oriented toward the blast, allow the nearly planar blast pressure to propagate progressively into the brain volume. This produces the coup-contrecoup features, modulated by the distance the wave must travel, shorter in the circle and longer for the composite shape. The flat surface of the composite model, when oriented toward the blast, allows the incident overpressure to propagate into the brain almost simultaneously across that surface. This propagation is relatively uniform in the brain and generates higher pressures and deeper penetration into the brain, highlighting the effect of local curvature.

Monte Carlo Results for Repetitive Blast Sequences

Using the database of 96 biomechanics simulations of 4 incident blast overpressures and 24 blast orientation angles, Monte Carlo simulations were conducted for 20 sequences of $N_{tot} = 200$ blasts for the three repetitive exposure environments—breacher training, mixed, and operational/combat environments.

Figure 11 shows an example CPEF plot exceeding the 142 kPa TBI threshold for a breacher sequence of 200 blasts.

Downloaded from https://academic.oup.com/milmed/article/185/Supplement_1/214/5740777 by guest on 19 April 2022

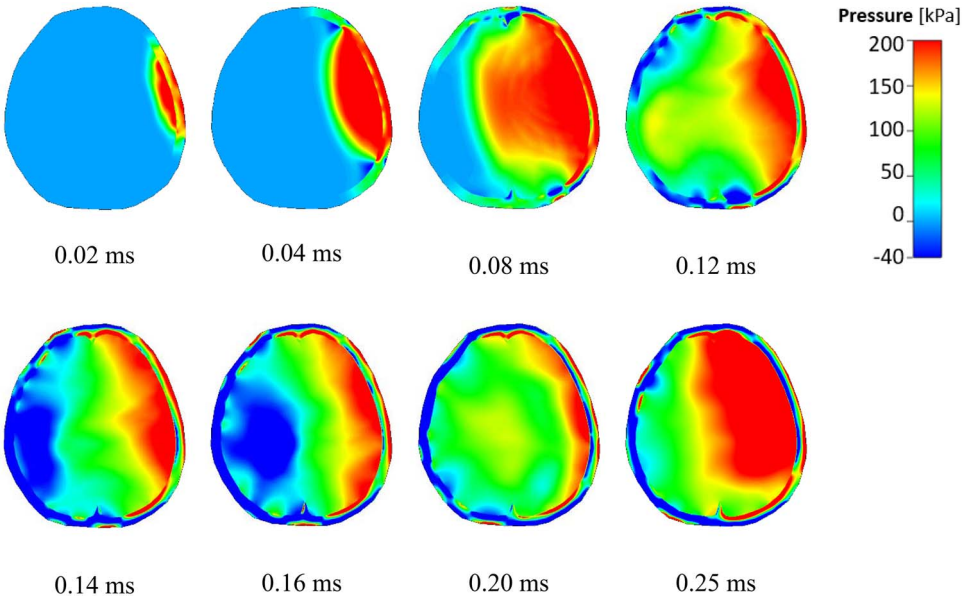


FIGURE 7. Dynamic pressures in head from single blast event at orientation angle of 75° and with incident overpressure of 15.0 psi (103 kPa).

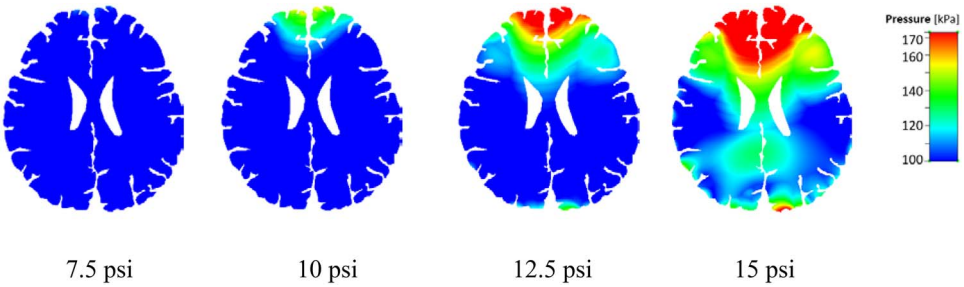


FIGURE 8. Maximum pressures in the brain from a single blast event at orientation angle of 0° and with incident overpressures of 7.5, 10.0, 12.5, and 15.0 psi (52, 69, 86, and 103 kPa), respectively.

It can be seen that in this training environment the predicted injury after repetitive blasts occurs at the front lobe of the brain, near the CSF-brain interface. Injury is very localized and CPEFs of 0.25 occur in a very small area. No injury is predicted when using higher TBI thresholds of 173 and 204 kPa.

Figure 12 shows a representative CPEF plot exceeding TBI thresholds of 142, 173, 204 kPa after a mixed sequence of 200 blasts. The CPEF map with the low injury threshold exceeds 0.25 across almost the entire model. The CPEF map generally decreases to approximately 15 and 5 percent with the higher injury thresholds. These CPEF levels also occur over large areas of the brain.

Figure 13 shows a representative CPEF plot exceeding TBI thresholds of 142, 173, and 204 kPa after an operational sequence of 200 blasts. The CPEFs are generally 17, 7, and 3% for the three injury thresholds. These results are generally higher than the breacher results because they contain more of the side blast orientations than the breacher results and also include some of the 15 psi (103.42 kPa) highest possible blast overpressures. They are generally lower than those of the mixed case results because they contain more of the back blast orientations, which effectively replace some of the more injurious side blasts.

To establish divergent and convergent behaviors across multiple sequences of blast events, the evolution of the CPEF parameter can be plotted for each of the 20 different random blast loading sequences ($N_{tot} = 200$) for each of the breacher, mixed, and operational exposures. Figure 14a shows the CPEF, in blue, exceeding TBI thresholds of 142 kPa changes with the increasing number of blasts. The cumulative mean and cumulative standard deviation (SD) are shown in red and black, respectively, in the semi-log plot of Figure 14b for the breacher sequence. There is no predicted injury when TBI thresholds of 173 and 204 kPa are used, so the cases are not plotted. In a similar style, Figures 15a–c and 16a–c show the CPEF, mean, and SD exceeding TBI thresholds of 142, 173, and 204 kPa with the increasing number of blasts. Figures 15d and 16d show the corresponding semi-log plots of mean and SD for the mixed and operational loading sequences.

Large fluctuations in the CPEF are present early in the individual random sequences as the variability associated with random overpressures and orientations is averaged over

Downloaded from https://academic.oup.com/milmed/article/185/Supplement_1/214/5740777 by guest on 19 April 2022

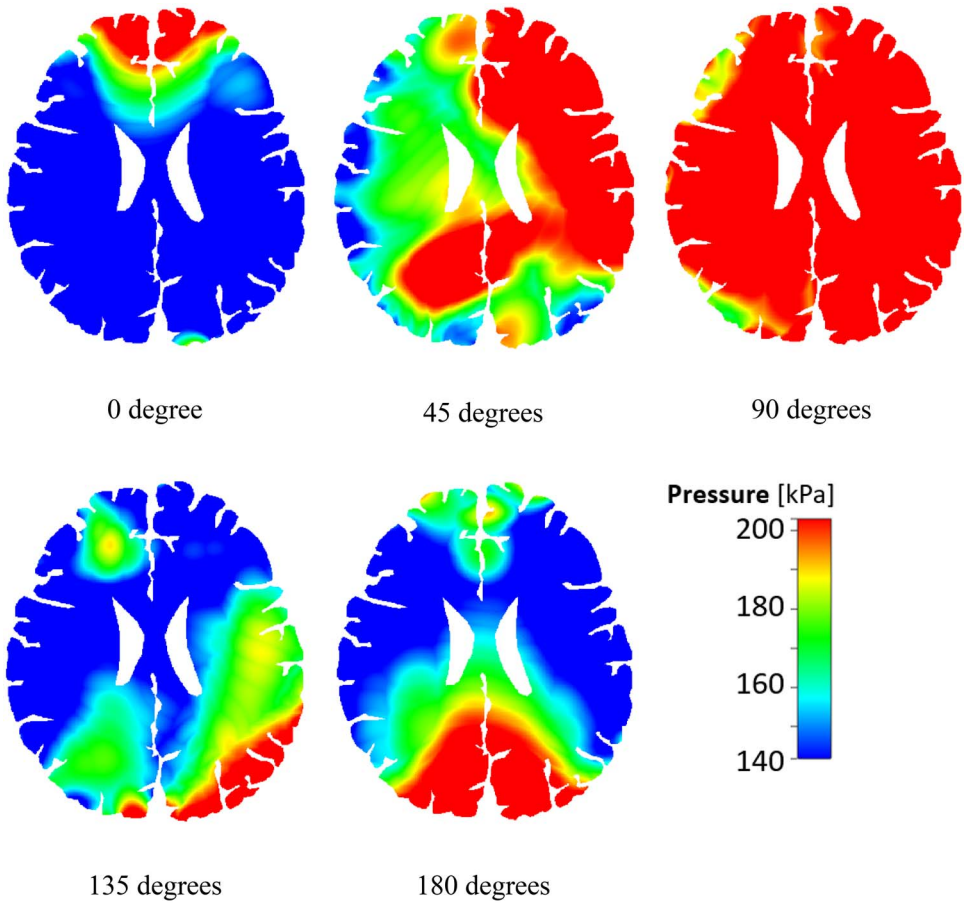


FIGURE 9. Maximum pressures in the brain from single blast event with incident overpressure of 15 psi (103 kPa) and at orientation angles of 0, 45, 90, 135 and 180°, respectively.

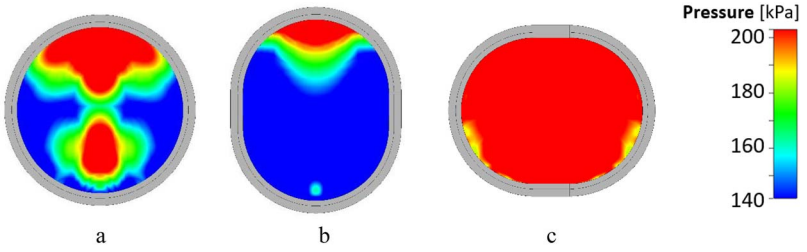


FIGURE 10. Maximum pressures experienced in the brain during blast loading of the (a) circular model, (b) composite shape model with a curved surface orientated at 0° in line with the blast, and (c) the composite shape model with a flat surface oriented at 0°in line with the blast.

relatively small numbers of blasts. As the number of blast events accumulates, the CPEF versus *N* curves for each blast sequence and TBI threshold converge toward a CPEF mean value with a residual CPEF SD.

Table IV summarizes the number of blasts to reach a "practical" equilibrium state for the mean values and residual SDs for each scenario. This equilibrium state is one in which each additional blast, while continuing to increase the cumulative exposure, does not significantly change these two quantities. However, even at 200 blasts, it is important to note that for each data set the 20 blast sequences have not reached a single mean value but are contained within a gradually narrowing band of values around the mean. Mean values stabilize between the first 30 and 60 blasts and SDs between the first 80 and 120 blasts. It is worth to note that the CPEF mean value in the mixed exposures converges at a higher number of blasts compared to the operational exposures, when using TBI thresholds of 173 and 204 kPa.

DISCUSSION

The results presented above provide insight into the way individual blast events expose the brain to higher pressures exceeding TBI thresholds. This information is used to describe

Downloaded from https://academic.oup.com/milmed/article/185/Supplement_1/214/5740777 by guest on 19 April 2022

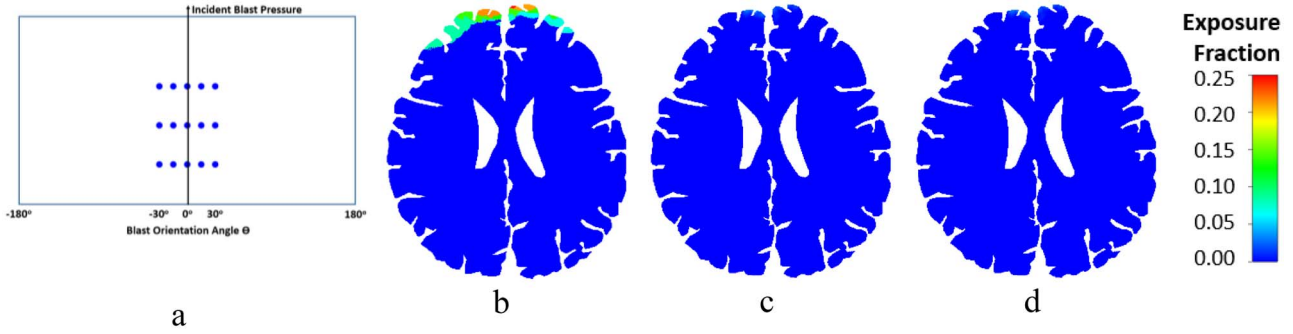


FIGURE 11. Example of Monte Carlo result for breacher sequence: (a) representative pressure-orientation distribution and (b–d) the CPEF(e, N_{tot}) exceeding TBI thresholds of 142, 173, and 204 kPa for $N_{\text{tot}} = 200$.

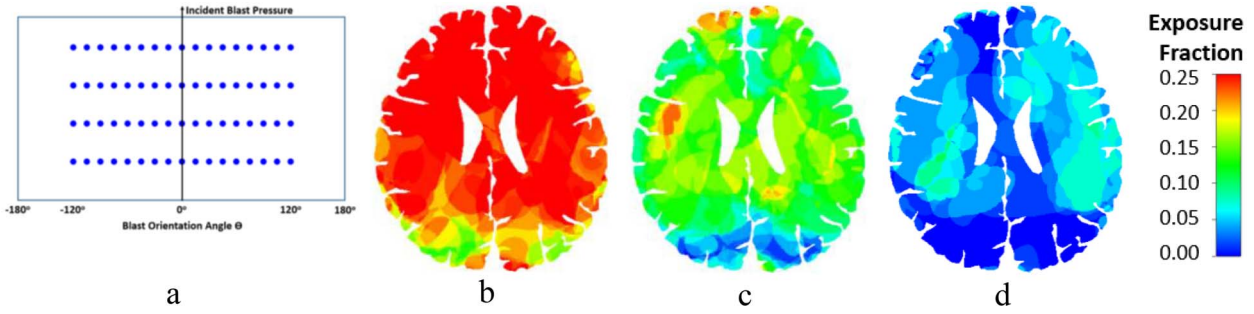


FIGURE 12. Example of Monte Carlo result for mixed sequence: (a) representative pressure-orientation distribution and (b–d) the CPEF(e, N_{tot}) exceeding TBI thresholds of 142, 173, and 204 kPa for $N_{\text{tot}} = 200$.

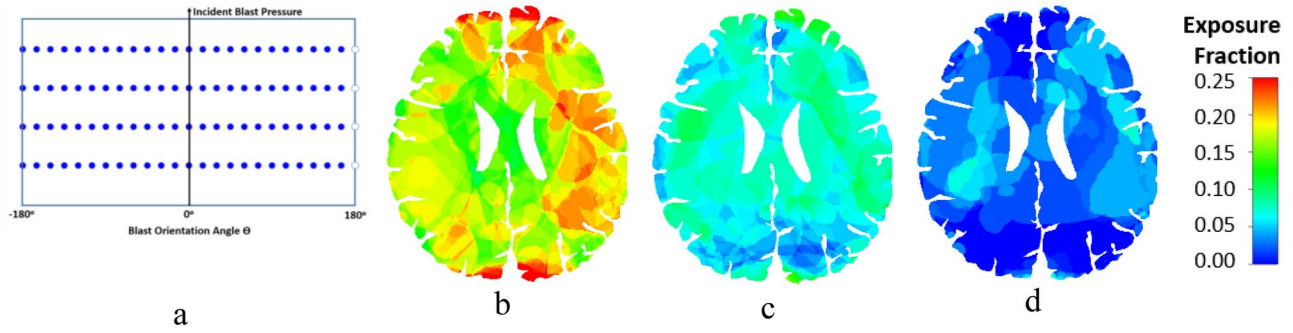


FIGURE 13. Example of Monte Carlo result for operational sequence: (a) pressure-orientation distribution and (b–d) the CPEF(e, N_{tot}) exceeding TBI thresholds of 142, 173, and 204 kPa for $N_{\text{tot}} = 200$.

how multiple blast event exposures are accumulated by the brain. Five different aspects of this study reinforce each other and quantify these trends.

First, the pressure versus time response across the brain from an individual blast is very heterogeneous. Pressure patterns vary strongly with both blast overpressure and blast orientation. The blast orientation effect is as influential as the blast magnitudes. For the same blast orientation, the higher blast overpressure causes larger brain model injury areas with higher pressures. For the same blast overpressure, blast from the side results in larger brain model injury areas than blast from other orientations.

Second, the maximum pressure encountered at each point in the brain from an individual blast creates complex patterns. This includes significant regions in these patterns beyond the coup and contrecoup locations. Especially for the side blasts, the affected area is much larger than the coup and contrecoup regions. The coup region, which is closer to the explosion source, is affected more than other regions. The higher pressure occurs in a smaller area in the contrecoup region compared to the coup region.

Third, a simplified analysis highlights the role of skull curvature in propagating incident blast overpressure into the brain. High skull curvature phases the contact of a planar or

Downloaded from https://academic.oup.com/milmed/article/185/Supplement_1/214/5740777 by guest on 19 April 2022

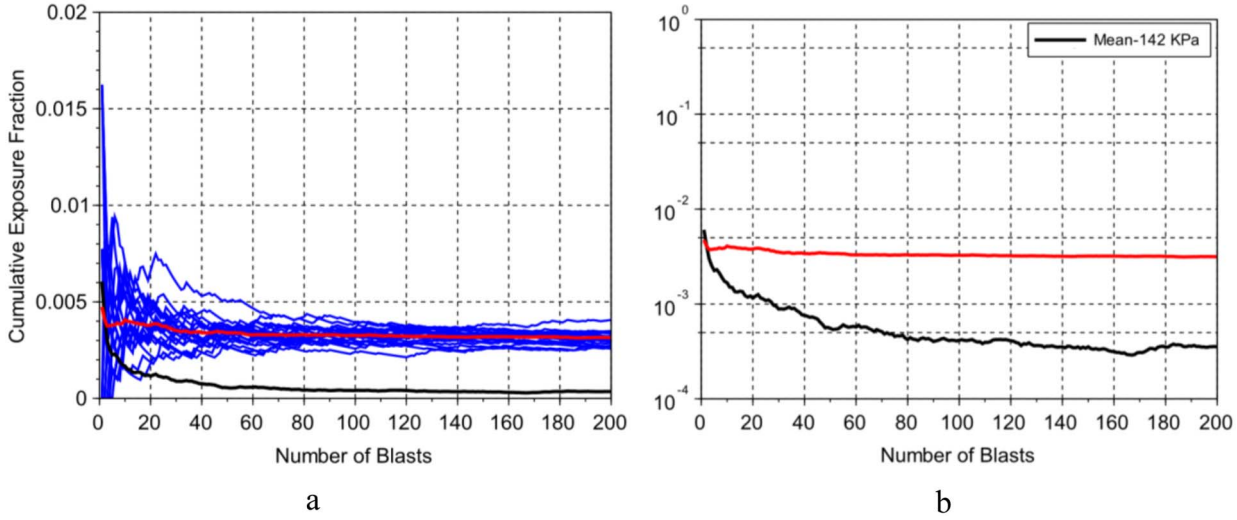


FIGURE 14. Monte Carlo results for breacher blast sequence: (a) CPEF(E_{tot}, N) exceeding TBI thresholds of 142 kPa and (b) semi-log plot of mean and SD with respect to number of blasts N. Cumulative mean value in red, cumulative SD in black.

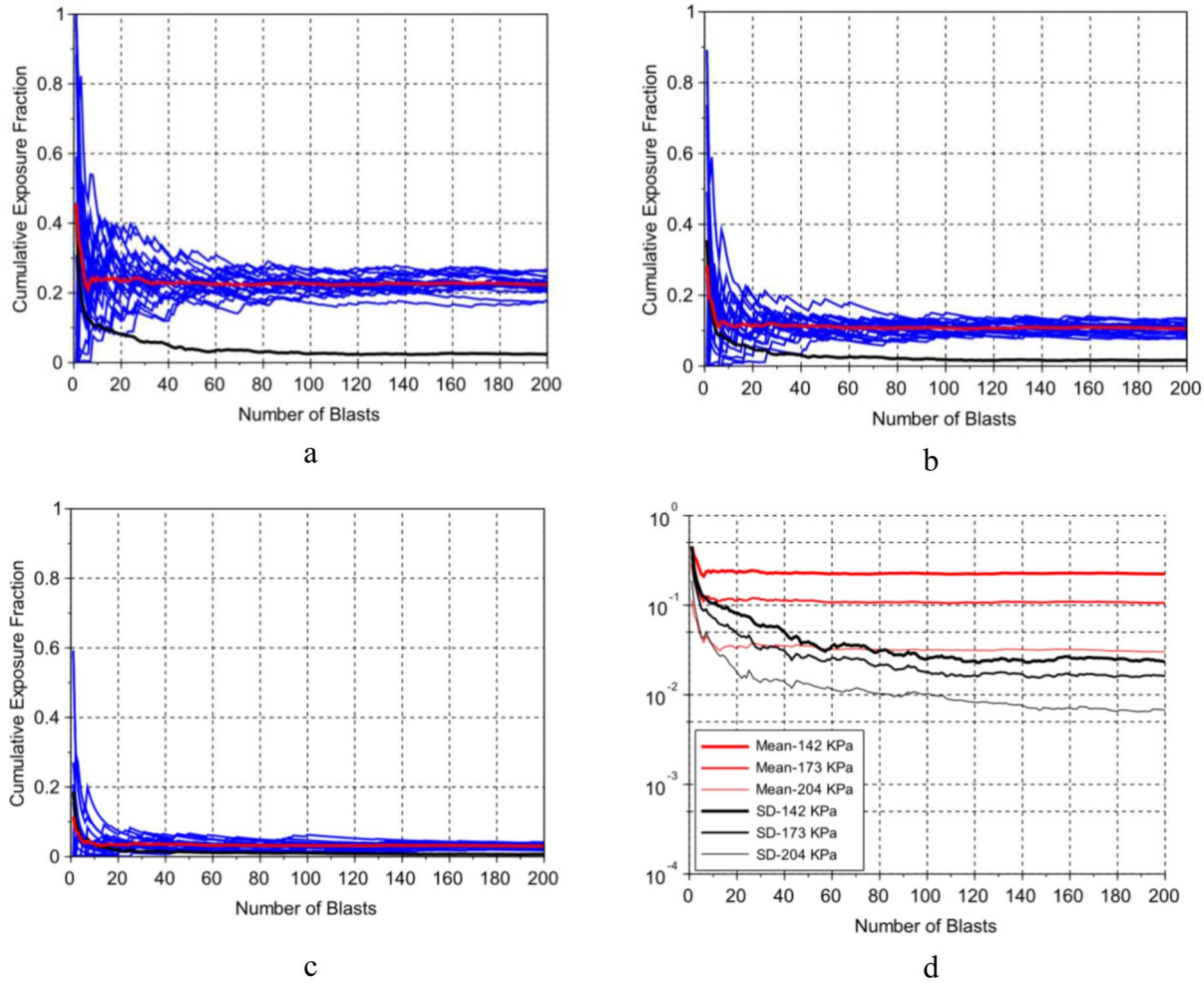


FIGURE 15. Monte Carlo results for mixed blast sequence: (a–c) CPEF(E_{tot}, N) exceeding TBI thresholds of 142, 173, and 204 kPa and (d) semi-log plot of mean and SD with respect to number of blasts N. Cumulative mean value in red and cumulative SD in black.

Downloaded from https://academic.oup.com/milmed/article/185/Supplement_1/214/5740777 by guest on 19 April 2022

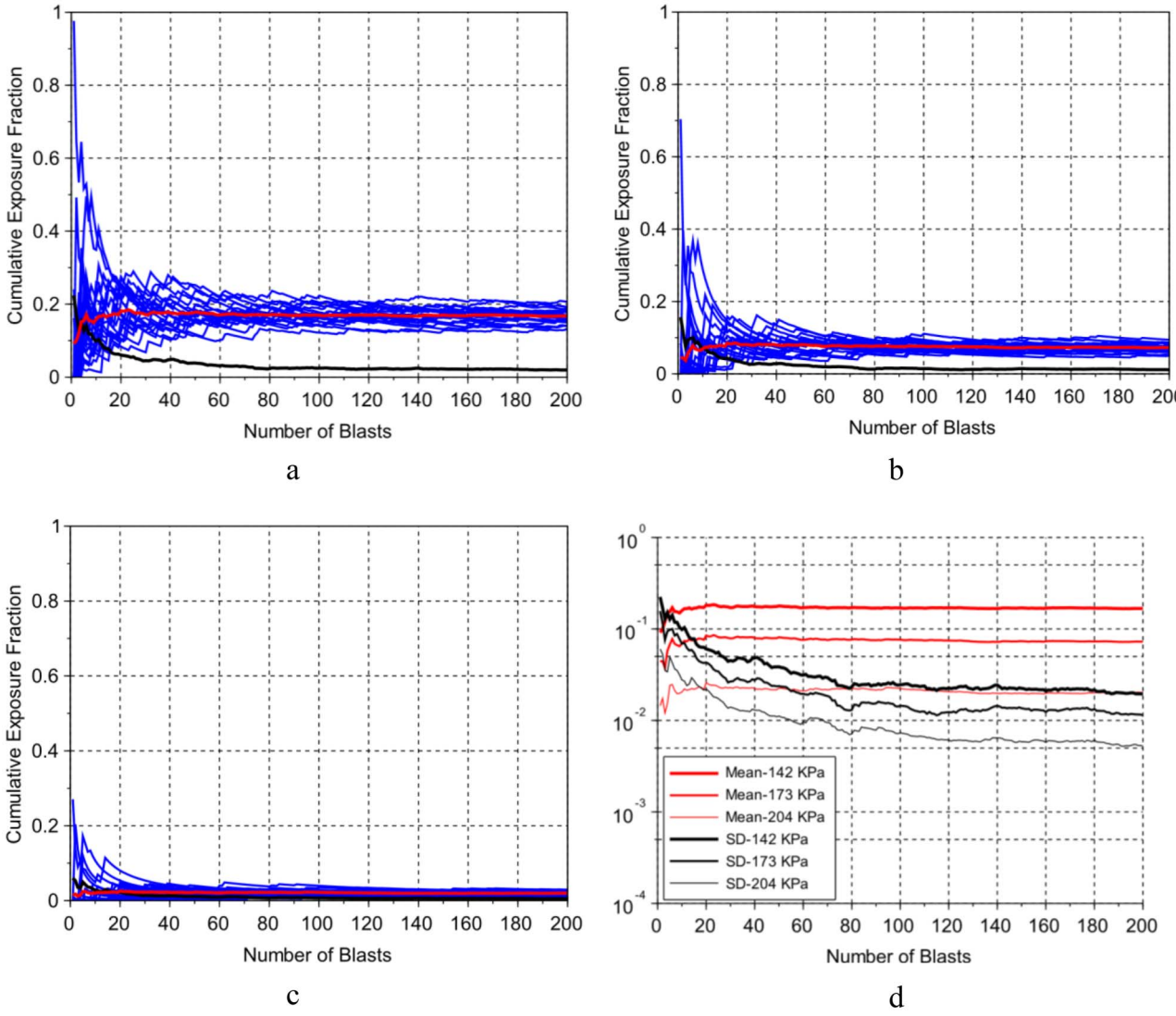


FIGURE 16. Monte Carlo results for operational blast sequence: (a–c) CPEF (E_{tot}, N) exceeding TBI thresholds of 142, 173, and 204 kPa and (d) semi-log plot of mean and SD with respect to number of blasts N. Cumulative mean value in red and cumulative SD in black.

nearly planar blast wave normal to the head. The propagation of pressure into the head proceeds nonuniformly with a curved wave front, allowing phased dynamic response of the brain. Low skull curvature allows a normal blast wave to contact the head over a large area nearly instantaneously, with propagation into the brain with a more linear wave front. This extends the findings by other researchers who noted that the side blast causes much higher pressure in the coup compared to the front one.[27,28]

Fourth, the CPEF quantifies those portions of the brain exceeding TBI thresholds. It tracks multiple blast exposures at each location in the brain and across the brain. It captures the complex geometric overlay patterns that develop from different blast overpressures and orientations, highlighting local regions of high and low cumulative exposure. It confirms that the local low skull curvatures on the left and right sides make the brain more susceptible to injury.

Fifth, the Monte Carlo simulations quantify the evolution of the CPEF, the cumulative mean, and cumulative SD versus number of blasts N. The CPEF itself is most sensitive, as shown by its fluctuations and range of responses at a lower N. The cumulative mean value is a more global measure of "dosing." Its convergence between approximately 30 and 60 blasts means that in the range of 0 to 30 blasts each CPEF pattern in the brain model is likely to be significantly different and changing in geometry and in magnitude. The cumulative SDs converge between the first 80 and 120 blasts meaning that in the range of 30 to 80 blasts the geometric details of the patterns in the brain will still be important and changing although the average total exposure will be similar.

Downloaded from https://academic.oup.com/milmed/article/185/Supplement_1/214/5740777 by guest on 19 April 2022

TABLE IV. Converged Values and Associated Numbers of Blasts for the Mean and SD of CPEF(E_{tot}, N_{tot})

CPEF(E_{tot}, N_{tot})	Breacher			Mixed			Operational		
	142 kPa	173 kPa	204 kPa	142 kPa	173 kPa	204 kPa	142 kPa	173 kPa	204 kPa
Mean	0.003	0	0	0.22	0.11	0.03	0.17	0.07	0.02
n_{mean}	56	—	—	35	59	60	32	40	40
SD	0.0004	0	0	0.020	0.016	0.007	0.020	0.010	0.005
n_{SD}	80	—	—	100	100	140	80	110	120

This paper highlights a problem and an approach to develop quantitative recommendations for military medicine by simulation and physical measures, which includes (1) characterizing loading domain in anticipated operational or training scenario bounds, (2) fusing intelligence and operational planning for area-specific threats, and (3) software prediction of CPEF ranges and convergence thresholds to guide forward command and medical decisions.

CONCLUSIONS

A systematic, quantitative, and practical characterization of cumulative exposure of the brain model to repetitive blast events was developed using computational simulation and a Monte Carlo probabilistic simulation. Results are generated in a computationally efficient manner for random blast sequences by constructing a detailed database, generated by a relatively small set of detailed biomechanics simulations, followed by a probabilistic analysis that tracks cumulative exposure from multiple blast events utilizing the database. This process is computationally extendable from this 2D model demonstration to the 3D analysis.

The results highlight and quantify the likely role of blast overpressures and orientations in random blast sequences on maximum pressure local values and spatial patterns across the brain. The associated mean values and SDs of the CPEF parameter, introduced to characterize the extent and repetition of high pressures exceeding different TBI thresholds, are tracked. Statistical convergence of the internal brain response metrics versus number and type of exposures quantitatively characterizes and highlights the different exposure sequences reflecting notional operational and training environments.

The significant variability in cumulative brain exposures in the early and intermediate portions of the repetitive blast sequences should be further analyzed and compared to the clinical variability of mTBI symptoms. The insights gained by this effort also complement and maximize the utility of orientation data from blast sensors worn by the warfighter.

FUNDING

This study was supported by the Office of Naval Research (ONR) through the Naval Research Laboratory's Basic Research Program and the Department of Defense (DOD) High Performance Computing Modernization Program at the Army Research Laboratory, Air Force Research Laboratory, and Army Engineer Research Laboratory DOD Supercomputing Resource Centers.

ACKNOWLEDGMENTS

The authors acknowledge Amit Bagchi from NRL for technical discussions on the blast scenarios and TBI thresholds.

REFERENCES

1. Heltemes KJ, Holbrook TL, Macgregor AJ, Galarneau MR: Blast-related mild traumatic brain injury is associated with a decline in self-rated health amongst U.S. military personnel. Injury 2012; 43: 1990–5.
2. Kamimori GH, Reilly LA, LaValle CR, Olaghere Da Silva UB: Occupational overpressure exposure of breachers and military personnel. Shock Waves 2017; 27: 837–47.
3. Brix KA, Brody DL, Grimes JB, et al: Military blast exposure and chronic neurodegeneration: summary of working groups and expert panel findings and recommendations. J Neurotrauma 2017; 34: S-18.
4. Bazarian JJ, Donnelly K, Peterson DR, Warner GC, Zhu T, Zhong J: The relation between posttraumatic stress disorder and mild traumatic brain injury acquired during operations enduring freedom and Iraqi freedom. J Head Trauma Rehabil 2013; 28(1): 1–12.
5. Trotter BB, Robinson ME, Milberg WP, McGlinchey RE, Salat DH: Military blast exposure, ageing and white matter integrity. Brain 2015; 138(Pt 8): 2278–92.
6. Courtney A, Courtney M: The complexity of biomechanics causing primary blast-induced traumatic brain injury: a review of potential mechanisms. Front Neurol 2015; 6: 221.
7. Cernak I: Understanding blast-induced neurotrauma: how far have we come? Concussion 2017; 2(3): .
8. Magnuson J, Leonessa F, Ling GS: Neuropathology of explosive blast traumatic brain injury. Curr Neurol Neurosci Rep 2012; 12(5): 570–9.
9. Kontos AP, Kotwal RS, Elbin RJ, et al: Residual effects of combat-related mild traumatic brain injury. J Neurotrauma 2013; 30(8): 680–6.
10. Carr W, Polejaeva E, Grome A, et al: Relation of repeated low-level blast exposure with symptomology similar to concussion. J Head Trauma Rehabil 2015; 30(1): 47–55.
11. Asken BM, Sullan MJ, DeKosky ST, Jaffee MS, Bauer RM: Research gaps and controversies in chronic traumatic encephalopathy: a review. JAMA Neurol 2017; 74(10): 1255–62.
12. Arciniegas DB, Anderson CA, Topkoff J, McAllister TW: Mild traumatic brain injury: a neuropsychiatric approach to diagnosis, evaluation, and treatment. Neuropsychiatr Dis Treat 2005; 1(4): 311–27.
13. Goldstein LE, Fisher AM, Tagge CA, et al: Chronic traumatic encephalopathy in blast-exposed military veterans and a blast neurotrauma mouse model. Sci Transl Med 2012; 4(134): 134ra60.
14. Hoge CW, McGurk D, Thomas JL, Cox AL, Engel CC, Castro CA: Mild traumatic brain injury in U.S. soldiers returning from Iraq. N Engl J Med 2008; 358(5): 453–63.

Downloaded from https://academic.oup.com/milmed/article/185/Supplement_1/214/5740777 by guest on 19 April 2022

15. McKee AC, Robinson ME: Military-related traumatic brain injury and neurodegeneration. Alzheimers Dement 2014; 10: S242–53.
16. Yeoh S, Bell ED, Monson KL: Distribution of blood-brain barrier disruption in primary blast injury. Ann Biomed Eng 2013; 41(10): 2206–14.
17. Meabon JS, Huber BR, Cross DJ, et al: Repetitive blast exposure in mice and combat veterans causes persistent cerebellar dysfunction. Sci Transl Med 2016; 8(321): 321ra6.
18. The Blast Gauge® System. Available at https://blastgauge.com/; accessed November 27, 2018.
19. Institute of Medicine. Gulf War and Health, Volume 9: Long-Term Effects of Blast Exposures. Washington, DC, National Academies Press, 2014.
20. Tan XG, Matic P: Blast pressure effects on the helmet shell, helmet pad, skull and brain system. Proceedings of 25th International Symposium on Military Aspects of Blast and Shock, Hague, Netherlands, 2018.
21. Saunders RN, Tan XG, Qidwai SM, Bagchi A: Towards identification of correspondence rules to relate traumatic brain injury in different species. Ann Biomed Eng 2018 doi: 10.1007/s10439-018-02157-1.
22. Saunders RN, Tan XG, Bagchi A: On the development of interspecies traumatic brain injury correspondence rules. J Mil Med 2019; 184: S181–94.
23. Brewick P, Teferra K: Uncertainty quantification for constitutive model calibration of brain tissue. J Mech Behav Biomed Mater 2018; 85: 237–55.
24. Tan XG, Przekwas AJ, Gupta RK: Computational modeling of blast wave interaction with a human body and assessment of traumatic brain injury. Shock Waves 2017; 27: 889–904.
25. Kingery CN, Bulmash G: Air-blast parameters from TNT spherical air burst and hemispherical surface burst, U.S. Army Ballistic Research Laboratory, Technical report BRL, 02555, 1984.
26. Rafaels KA, Bass CR, Panzer MB, et al: Brain injury risk from primary blast. J Trauma Acute Care Surg 2012; 73(4): 895–901.
27. Hua Y, Wang Y, Gu L: Primary blast waves induced brain dynamics influenced by head orientations. Biomed Eng Lett 2017; 7(3): 253–9.
28. Haniff S, Taylor PA: *In-silico* investigation of blast-induced intracranial fluid cavitation as it potentially leads to traumatic brain injury. Shock Waves 2018; 27(6): 929–45.

Downloaded from https://academic.oup.com/milmed/article/185/Supplement_1/214/5740777 by guest on 19 April 2022